Sequential Formation of Natrolite-Group Zeolites In Amygdules of Basaltic Lavas

Article *in* The Canadian Mineralogist · July 2015

DOI: 10.3749/canmin.1500036

2 authors:

Sevgi Özen
Recep Tayyip Erdoğan Üniversitesi
8 PUBLICATIONS **60** CITATIONS
SEE PROFILE

M. Cemal Göncüoğlu
Middle East Technical University
464 PUBLICATIONS **7,778** CITATIONS
SEE PROFILE

The Canadian Mineralogist
Vol. 53, pp. 757-765 (2015)
DOI: 10.3749/canmin.1500036

SEQUENTIAL FORMATION OF NATROLITE-GROUP ZEOLITES IN AMYGDULES OF BASALTIC LAVAS

SEVGI ÖZEN[§]

Recep Tayyip Erdoğan University, Industrial Design Engineering, 53000 Fener-Rize, Turkey

M. CEMAL GÖNCÜOĞLU

Middle East Technical University, Geological Engineering Department, Ankara, Turkey

ABSTRACT

Natrolite-group minerals were found in amygdules in Middle Eocene basaltic lavas in northern central Anatolia and have been evaluated in detail by petrographical, mineralogical, and chemical studies. A sequential formation of zeolites, which occurred in response to the interaction of the host rock with heated water, was determined by examination of the mineral assemblage. The compounds necessary for the formation of secondary minerals might have been derived from alteration of volcanic glass and Ca-rich pyroxenes in the host rock as well as from the associated marine sediments. Formation of fibrous zeolites on the walls of the amygdules began with a Na-rich zeolite, followed by a progressive increase in Ca content, and ended with a Ca-rich zeolite. The growth of natrolite as the earliest phase starts around an unidentified nucleus. It is followed by mesolite, which forms epitaxial overgrowths with natrolite. Scolecite is the last zeolite in the crystallization sequence. A continuous increase of the Si/Al ratio is observed from the earlier phase towards the later ones. The latest phase occupying the cavities within the amygdules is calcite.

Keywords: natrolite, mesolite, scolecite, amygdaloidal, sequence of crystallization, basaltic lava.

INTRODUCTION

Large attractive crystals of zeolites admired by mineral collectors occur very commonly in amygdules in volcanic rocks, particularly in basaltic lava flows. These zeolites commonly belong to the natrolite group and were first identified by Klaproth (1803) from the Hegau volcanic field, Germany (Gottardi & Galli 1985). The natrolite-group zeolites consist of an aluminosilicate framework made up of 4-1 ring units of $(Si,Al)O_4$ tetrahedra, running parallel to the **c**-axis (Gottardi & Galli 1985, Tsitsishvili *et al.* 1992, Passaglia & Sheppard 2001, Armbruster & Gunter 2001). Since needle-like and fibrous crystals elongated parallel to the tetrahedral chains are common, this group of zeolites is often described as "fibrous zeolites" (Gottardi & Galli 1985). Three subgroups are described as three different framework topologies, based on the cross-linking of the tetrahedral chains (Armbruster & Gunter 2001). These are the natrolite group (NAT) (natrolite, mesolite, scolecite, paranatrolite, and gonnardite), thomsonite (THO), and edingtonite (EDI) (edingtonite, kalborsite). Sodium and Ca are the dominant cations in this group (Armbruster & Gunter 2001). Natrolite ($Na_{16}Al_{16}Si_{24}O_{80} \cdot 16H_2O$) is a Na-rich variety with small amounts of Ca and K, and trace amounts of Mg, Sr, and Ba (Alberti *et al.* 1982). Mesolite ($Na_{16}Ca_{16}Al_{48}Si_{72}O_{240} \cdot 64H_2O$) is intermediate in chemical composition between natrolite and scolecite. Scolecite ($Ca_8Al_{16}Si_{24}O_{80} \cdot 24H_2O$) is always Ca-rich, with only minor amounts of Na and traces of K.

In this study, we will report the petrographic and geochemical features of fibrous zeolites within spherical amygdules, up to 25 mm in diameter within basaltic lava flows in northern Central Anatolia around Sorgun. The aim of this study is to identify the zeolite minerals using combined analytical techniques, to determine their order of crystallization, and to discuss their mode of formation.

GEOLOGICAL SETTING

The volcanic rocks with the zeolite-rich amygdules are located within the Middle Eocene (Göncüoğlu 2010) volcanic and volcanoclastic rocks of the Yozgat-Sorgun Tertiary basin (Fig. 1). They are mainly subaqueous lava flows and subareal domes, concentrated along the basin

[§] *Corresponding author e-mail address*: sevgi.ozen@erdogan.edu.tr

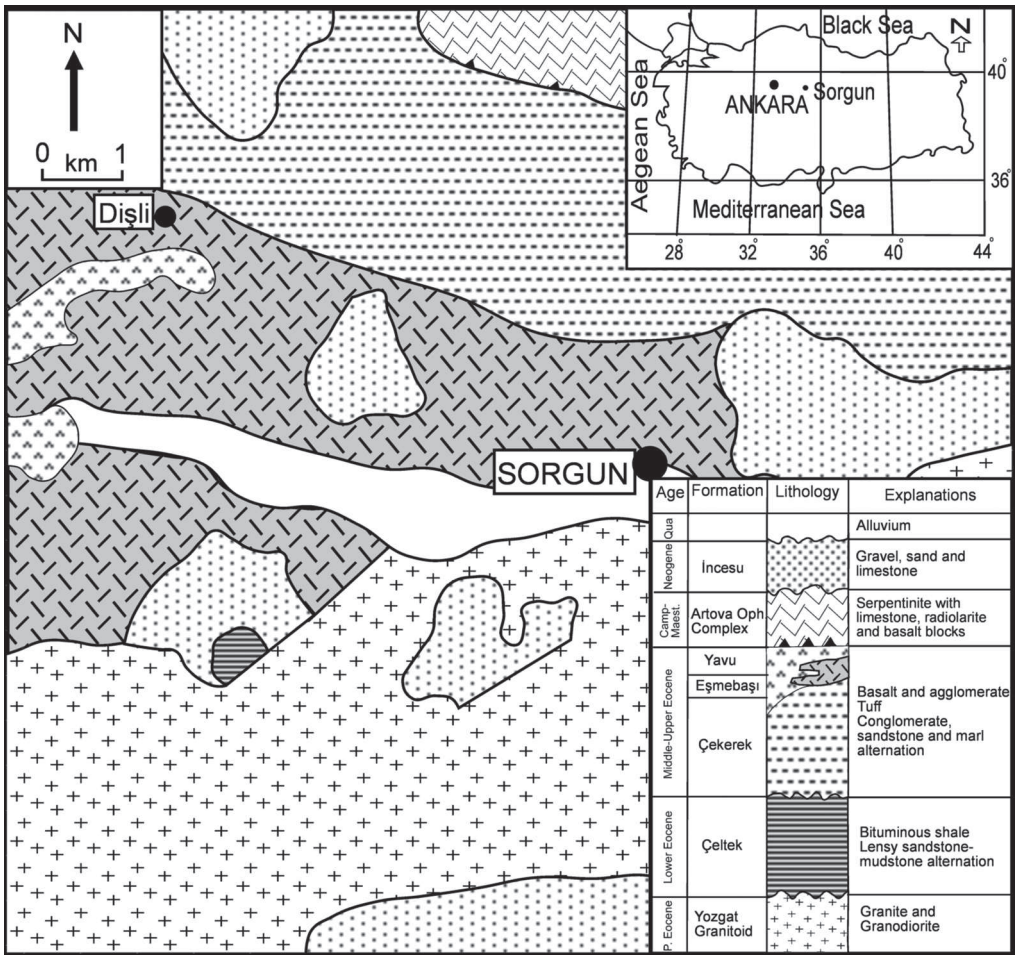

FIG. 1. Simplified geological map of the Sorgun (Yozgat) area (after Karayiğit *et al*. 1996).

and associated with wide-spread Middle Eocene (Bartonian) volcanism (Karayiğit *et al*. 1996, Alpaslan & Temel 2000, Geneli *et al.* 2010). The lavas are basic to intermediate in composition (Göncüoğlu & Geneli 2008) and are classified as basalt, basaltic andesite, and rarely as alkali basalt and trachyandesite (the Bayat Volcanics of Erdoğan *et al.* 1996). The lavas flows are pillowed to massive and attain 5 m in thickness. They are interbedded with clastic-volcanoclastic sequences and limestones with shallow-marine fossils. The dominant volcanic rock-types are highly amygdaloidal basalts and basaltic andesites, either black or dark grey in color. The margins of the pillows are characterized by dark brown spherical amygdules with decreasing radii towards the center of the pillows. The average size of the amygdules is 5–7 mm, but they attain 20–25 mm in diameter. On the fresh surface, the interior of the amygdule is characterized by fine natrolite-group minerals occurring as fan-like interpenetrating aggregates of vitreous, white to pinkish prismatic crystals.

ANALYTICAL METHODS

Representative hand specimens were selected from the field to examine in the laboratory. Thin sections were first examined with an optical microscope to determine the petrographic properties of the amygdule minerals and their textural relations from rim to core. Thin section investigations were performed using a Nikon polarizing microscope and photomicrographs were taken using an image analyzer system attached to a Nikon camera. X-ray powder diffraction (XRD) analyses were conducted using a Rigaku MiniFlex II X-ray diffractometer with a Cu$K\alpha$ source operating at 30 kV and 15 mA with a scan rate of 10 degree/min in the range of 0–40° to confirm the identity of the zeolite minerals. All powdered samples were prepared with an agate mortar. The observed *d*-spacings on the XRD patterns were compared with JCPDS reference patterns. Petrographic and XRD studies were performed in the laboratory of the Geological Engineering Department of

the Middle East Technical University (METU), Turkey. Mineral textures, crystal relationships, and morphological characteristics of secondary minerals were analyzed from gold-coated samples with a JEOL 6400 SEM at the Central Laboratory at METU. The SEM analyses were performed on the same samples used for the petrographic and XRD studies. Compositional analyses in wavelength-dispersive mode were performed using polished thin sections and a JEOL JXA 8200 electron microprobe at the Department of Earth Sciences, University of Milan, Italy. The system was operated with an accelerating voltage of 15 kV, a beam current of 5 nA, and a counting time of 30 s on the peaks and 10 s on the background. A defocused beam (Ø 10 μm) was used to minimize the loss of water due to the electron bombardment. A series of minerals (*i.e.*, wollastonite for Si, anorthite for Ca and Al, K-feldspar for K, forsterite for Mg, fayalite for Fe, omphacite for Na, sanbornite for Ba, and celestine for Sr) were used as standards. The results were corrected for matrix effects using a conventional ZAF routine in the JEOL suite of programs (Tingle *et al.* 1996). The reliability of the analysis is confirmed by the low balance error E<7, where E% (Passaglia 1970) is 100X [Al − (Na + K) − 2(Mg + Ca + Sr + Ba)]/[(Na + K) + 2(Mg + Ca + Sr+Ba)].

Results

Petrographic Observations

Petrographically, the studied basaltic rocks display features typical of the Bayat Volcanics, as previously described by Büyükönal (1986), Alpaslan & Temel (2000), and Geneli (2011). Thin section studies indicate that the rock with the amygdules is fine-grained porphyritic basalt, which comprises mainly olivine phenocrysts with smaller amounts of Ca-clinopyroxene, orthopyroxene, and minor biotite as mafic constituents. Labradoritic plagioclase occurs as zoned phenocrysts as well as microliths. Accessory phases are Fe-Ti oxides and titanite. The texture of the groundmass ranges from hypocrystalline to holocrystalline and its microphenocryst content is similar to that of the phenocryst assemblage. In general, it comprises subhedral microlitic plagioclase, clinopyroxene, volcanic glass, and minor Fe-Ti oxides in the groundmass.

In some samples, the glassy matrix displays perlitic cracking indicating hydration. Most of the studied samples display various degrees of alteration. The alteration is especially dominant at the rim of the pillows and includes calcite, clay minerals replacing plagioclase, iddingsite and serpentine replacing olivine, and chlorite replacing clinopyroxene. The larger and corroded Ca-plagioclase crystals altered preferentially. In such cases, alteration proceeds from the margin along some cracks and affects the innermost zones of the phenocrystic plagioclases. In several cases these larger phenocrysts are completely replaced by coarse-grained calcite. The micro-phenocrysts in the glassy matrix, on the other hand, are only altered along the rims. Based on optical determination the clinopyroxenes are augites. They are variably altered along rims and cleavage planes. As is the case in plagioclase phenocrysts, the diopsitic core of the weakly zoned clinopyroxenes is highly altered.

The degree of vesiculation increases towards the rims of the pillows and at the rims of massive lava flows in contact with the sedimentary rocks. These cavities are mainly filled with secondary zeolites and calcite. Less frequently, amygdules filled with quartz are observed.

For identification of the zeolites, especially natrolite, mesolite, and scolecite, petrographic examination has proved to be the most practical method because of the easier sample preparation, rapid identification, and reliability (Gunter & Ribbe 1993). The simplest way to differentiate between these three minerals is to determine their birefringence, sign of elongation, and isotropism. Natrolite is always length-slow, mesolite seems near isotropic, and scolecite is always length-fast (Gunter & Ribbe 1993, Gunter *et al.* 1993). Therefore, detailed petrographic examination of a number of thin sections of larger amygdules was used for discrimination of natrolite, mesolite, and scolecite.

Optical properties indicate that the amygdules in the host rock were gradually filled up with secondary mineral phases from the outer wall to the center, developing three mineral zones (Fig. 2). Natrolite-group crystals vary from 3 to 20 mm in length and 0.1 to 0.25 mm in thickness. They occur as prismatic radial aggregates growing inwards from the amygdule walls with an unidentified nucleus (Fig. 3a) and are crosscut towards the cavity center by each other (Fig. 3b). Fan-like crystals in Zone I exhibit low birefringence (first-order yellow to orange), and are colorless with parallel extinction (Fig. 3a, b). These crystals were identified as natrolite because they are always length-slow. Towards the middle part of the prismatic crystal (Zone II), isotropic mesolite can be distinguished from natrolite (Fig. 3c). The edges of the isotropic mesolite are altered by natrolite as shown in Figure 3d. The optical properties used to distinguish them from mesolite are the yellow birefringence, parallel extinction, and positive sign of elongation. In this part (Zone II) scolecite also occurs as a precipitation mineral around mesolite prisms. Scolecite is the last natrolite-group mineral to form in the cavities, and it usually occurs together with calcite. At the edge of the crystal (Zone III) in the center of the amygdule, mesolite crystals are isotropic in thin section cut parallel to {110}. The crystals cut parallel to {001} show light and dark contrast (Fig. 3e, f), which is related to the parallel intergrowths akin to (110) twinning as described by Akizuki & Harada (1988). The short axis of mesolite parallel to the elongation is recognized as the **c**-axis (*e.g.*, Nawaz *et al.* 1985). In the center of the amygdule, natrolite-group crystals are completely surrounded by colorless calcite with high birefringence and evident cleavage (Fig. 3e, f). Some calcite grains are twinned.

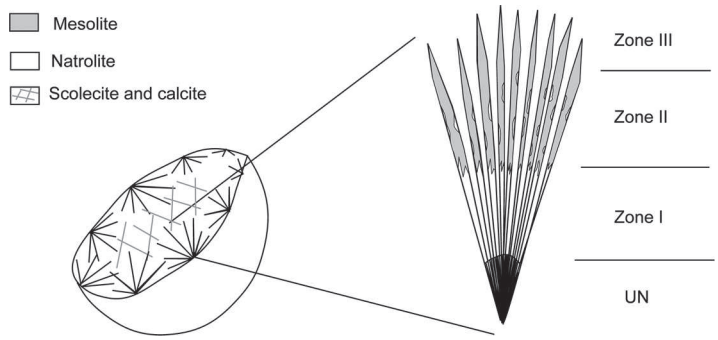

FIG. 2. Schematic sketch illustrating the textures and zones of natrolites filling the amygdules (UN = unidentified nucleus).

X-ray powder diffraction (XRD)

According to the XRD patterns of the studied samples, natrolite-group minerals are the major component. The reflections at 13.54, 15.06, 19.02, 20.26, and 31.22 °2θ with *d*-spacings of 6.54, 5.88, 4.66, 4.38, and 2.86 Å are the most distinctive. Minor amounts of calcite are recognized by the *d*-spacing of 3.03 Å. Analcime recorded as an accessory mineral was distinguished from the members of the natrolite group by the reflections at 5.61, 3.43, 2.89, and 2.51 Å.

Scanning electron microscopy (SEM)

Scanning electron microscopy micrographs of cavity-filling natrolite group crystals are shown in Figure 4. Epitaxial natrolite-mesolite overgrowths are arranged in fan-shaped or radial aggregates. Their length varies in size from 2 to10 mm and their width from 0.5 to 20 μm. Scanning electron microscopy images clearly show that they nucleated at the walls of the cavities and developed from there towards the center (Fig. 4a). They are recognized by their typical prismatic habit and well-formed {110} crystal faces (Fig. 4b). The composition of the earliest-formed zeolite phase at the cavity-wall (nucleus) could not be identified (Fig. 4c). An enlargement of Figure 4c only shows small analcime crystals, recognized by their trapezohedral morphology, which attain 2 μm in diameter (Fig. 4d).

Chemical composition

The chemical compositions of the large cavity-filling zeolites determined by electron microprobe are reported in Table 1. Polished thin sections were made from Zone II and Zone III. The microprobe analyses of the zeolite samples appear to be reliable, as E%, *i.e.*, the charge balance between aluminum and extra-framework cations, is within 7%. On the basis of the EPMA data, the zeolites present are natrolite, mesolite, and scolecite, which are well-known endmembers of the natrolite group (Gottardi & Galli 1985). Sodium is the most dominant extra-framework cation in natrolite (Table 1). The CaO content is low, which is a common feature in many natrolites (Birch 1989). Only trace amounts of K were detected. Iron and Sr are either absent or very low in the studied natrolite samples. The Si/Al ratio of the natrolite ranges between 1.48 and 1.50. Mesolite has very low amounts of cation contents other than Ca and Na. The chemical composition of K-free mesolite shows that the Ca and Na contents range from 5.16–5.29 and 4.85–5.12, respectively. The Si/Al ratio varies from 1.49 to 1.52. Scolecite is dominated by Ca, which attains 5.56 atoms per formula unit (*apfu*), and Na only occurs in minor amounts. The K content varies between 0.91 and 1.37 *apfu*. Strontium, Ba, Mg, and Fe are present in trace amounts in the structure of this mineral. Scolecite, as a matter of fact, has a higher Si/Al ratio than natrolite and mesolite with an average of 2.11, which indicates that the Si/Al ratio increases as the zeolitization process advances. Back-scattered electron images show that the partial transformation of mesolite to natrolite occurs as rims around the mesolite cores. This feature is typical for Zone II, as was also seen in the petrographic analysis (Fig. 5a). In Zone III in the center of the amygdule, only mesolite crystals are seen (Fig. 5b).

DISCUSSION AND CONCLUSIONS

In nature, zeolites occur over a wide range of temperatures (4 to 250 °C) and with a wide variety of structures in aqueous environments (Breck 1974, Gottardi & Galli 1985, Tschernich 1992). Most zeolites can crystallize in different geological environments such as saline-alkaline lakes, soil and surfacial deposits, and sea-floor sediments, or by processes such as hydrothermal alteration, burial metamorphism, *etc.* (Boles & Coombs 1977, Hay 1978, Mumpton 1978, Gottardi 1989, Ming & Mumpton 1989, Hay & Sheppard 2001). In addition, fibrous zeolites can form from cooling of volcanic flows as in the studied case. In

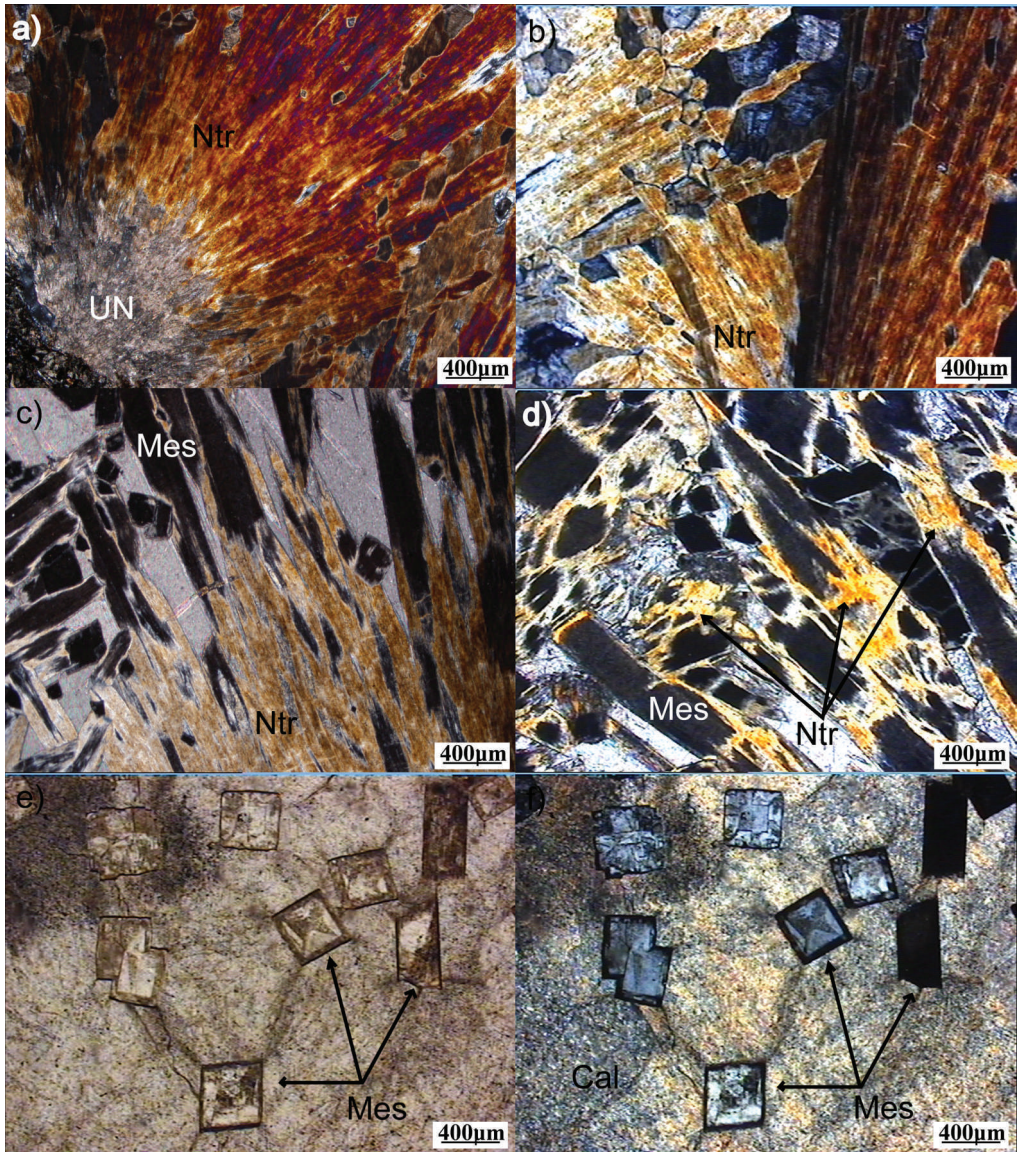

FIG. 3. Photomicrographs showing the occurrence of natrolite- group minerals in the amygdules. (a) Characteristic fan-like natrolite crystals are growing on amygdule walls with unidentified nucleus; (b) natrolite crystals crosscutting each other and exhibiting first-order orange birefringence; (c) isotropic mesolite is epitaxially intergrown with natrolite; (d) isotropic mesolite replaced by natrolite; (e) mesolite crystals cut parallel to {110} are isotropic and crystals cut parallel to {001} shows light and dark contrasts; (f) XPL view of (e) (UN = unidentified nucleus, Ntr = natrolite, Mes = mesolite, Cal = calcite).

lava-flows in aqueous environments, as evidenced by the presence of pillows, the molten volcanic rock comes into contact with water. The rapid cooling at the surface of the flow results in the formation of a fine-grained chilled margin, which prevents the escape of the dissolved gas-content of the lava, resulting in the formation of vesicles. On the other hand, the interaction of water with the hot lava increases the temperature of the water and accelerates the hydrolysis mechanism and dissolution. This process causes leaching of the ions needed for zeolite formation from highly reactive phases. The vesicles might have provided both circulatory pathways for heated solutions and spaces for fine zeolite crystallization. According to Tschernich (1992), the glassy basement of the flow is much more easily dissolved than the inner part of the microcrystalline host

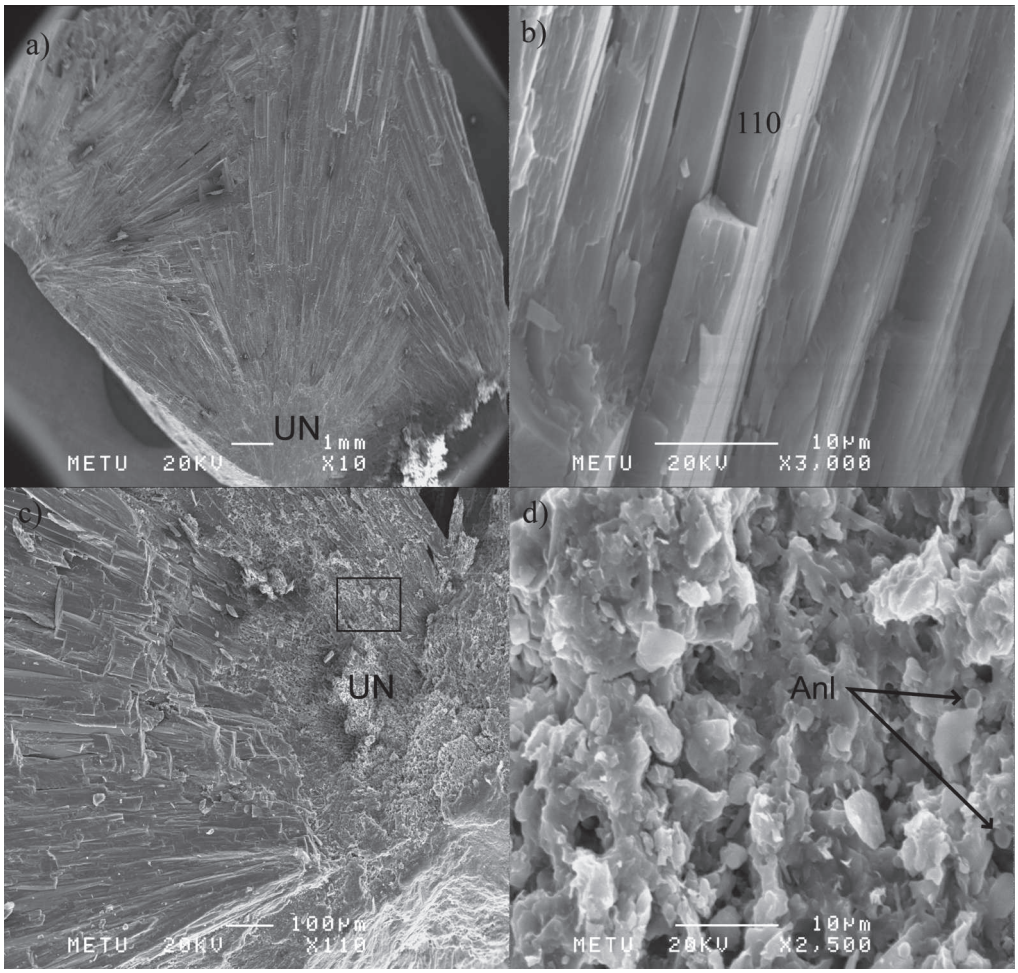

FIG. 4. SEM micrographs showing (a) fan-like interpenetrating aggregates of natrolite-mesolite overgrowths; (b) prismatic natrolite group minerals recognized with well-formed {110} faces; (c) unidentified nucleus; (d) magnified view of the unidentified nucleus. Trapezohedral analcime crystals are seen (UN = unidentified nucleus, Anl = analcime).

rock. The formation of zeolites is controlled by various agents, including chemical composition of the host rock, temperature-pressure conditions, circulation of solutions, fluid composition, *etc*. (Kristmannsdottir & Tomasson 1978).

In the present study, the types and order of crystallization of the zeolites were demonstrated by examining the mineral assemblage in amygdules from a basaltic flow in a shallow-marine environment. From petrographic and chemical analyses of the zeolite minerals, it can be suggested that the composition of the vesicle-filling solutions was suitable to precipitate first a Na-rich zeolite, namely natrolite, where Na^+ might have been provided by alteration of volcanic glass. With gradual change in fluid composition during crystal growth, mesolite becomes the stable phase, and it grew epitaxially on natrolite. The same kind of epitaxial natrolite-mesolite overgrowths were reported by Tschernich (1992) in Oregon, USA. Thin-section observations revealed that scolecite seems to form in the amygdule after mesolite crystallization. Precipitation of anhedral scolecite around fine prismatic mesolite crystals is indicative of the last generation of zeolite formation. Enrichment of the crystallizing solution in Ca^{2+} may be due to the alteration of Ca-rich pyroxene in the host rock. Thus for a considerable time thereafter, the saturated solution might have been responsible for the crystallization of scolecite. While scolecite crystallizes, decreasing Ca^{2+} in solution led to the partial replacement of the edges of the mesolite crystals by natrolite. Calcite is the last mineral to form, and it fills the center of the amygdule. Precipitation of calcite suggests that the late fluids might have interacted with calcareous sedimentary rocks. In addition, the

TABLE 1. CHEMICAL ANALYSES OF NATROLITE MINERAL GROUP

Region	Zone II															Zone III			
Analysis No.	1	2	3	4	5	6	7	8	9	10	11	12	13	14	15	16	17	18	19
Mineral	scolecite	scolecite	scolecite	mesolite	mesolite	mesolite	mesolite	mesolite	mesolite	mesolite	natrolite	natrolite	natrolite	natrolite	natrolite	mesolite	mesolite	mesolite	mesolite
SiO_2 wt.%	53.38	53.37	53.09	46.04	45.85	46.00	46.07	45.87	46.38	46.43	46.88	47.14	47.36	47.07	46.89	46.14	46.07	46.28	46.02
Al_2O_3	21.46	21.48	21.41	25.81	26.07	25.74	25.72	26.07	26.07	26.06	26.83	26.66	26.75	26.89	26.92	25.89	25.95	26.01	26.07
Fe_2O_3	0.02	0.01	0.02	0.00	0.00	0.00	0.00	0.02	0.00	0.03	0.03	0.00	0.00	0.01	0.00	0.04	0.00	0.00	0.00
MgO	0.02	0.02	0.00	0.00	0.01	0.00	0.00	0.00	0.00	0.00	0.00	0.00	0.00	0.00	0.00	0.00	0.00	0.00	0.02
CaO	10.07	9.35	10.17	9.22	9.28	9.31	9.28	9.46	9.34	9.36	0.20	0.23	0.29	0.74	0.12	9.35	9.22	9.37	9.29
Na_2O	0.57	0.98	0.49	5.02	4.99	4.79	5.04	5.05	4.92	5.01	15.31	14.77	14.99	14.42	15.26	4.92	4.80	4.80	4.99
K_2O	1.41	2.12	1.41	0.00	0.00	0.00	0.00	0.00	0.00	0.01	0.02	0.01	0.02	0.01	0.04	0.01	0.00	0.00	0.00
BaO	0.00	0.02	0.00	0.00	0.01	0.10	0.09	0.00	0.07	0.04	0.00	0.00	0.00	0.00	0.00	0.00	0.00	0.04	0.00
SrO	0.04	0.00	0.04	0.00	0.00	0.15	0.02	0.00	0.03	0.00	0.05	0.11	0.00	0.00	0.00	0.00	0.00	0.00	0.00
H_2O	13.04	12.65	13.37	13.91	13.79	13.91	13.77	13.53	13.19	13.06	10.68	11.07	10.59	10.85	10.77	13.65	13.96	13.49	13.61
Total	100.00	100.00	100.00	100.00	100.00	100.00	100.00	100.00	100.00	100.00	100.00	100.00	100.00	100.00	100.00	100.00	100.00	100.00	100.00
Atomic proportions on the basis of 40 Si+Al *apfu*																			
Si	27.14	27.13	27.11	24.09	23.95	24.10	24.13	23.96	24.06	24.08	23.89	24.00	24.01	23.91	23.86	24.08	24.04	24.06	23.99
Al	12.86	12.87	12.89	15.91	16.05	15.90	15.87	16.04	15.94	15.92	16.11	16.00	15.99	16.09	16.14	15.92	15.96	15.94	16.01
Fe^{3+}	0.01	0.01	0.01	0.00	0.00	0.00	0.00	0.01	0.00	0.01	0.01	0.00	0.00	0.00	0.00	0.02	0.00	0.00	0.00
Mg	0.01	0.02	0.00	0.00	0.01	0.00	0.00	0.00	0.00	0.00	0.00	0.00	0.00	0.00	0.00	0.00	0.00	0.00	0.02
Ca	5.49	5.09	5.56	5.17	5.19	5.23	5.21	5.29	5.19	5.20	0.11	0.13	0.16	0.40	0.07	5.23	5.16	5.22	5.19
Na	0.57	0.96	0.49	5.10	5.06	4.87	5.12	5.12	4.96	5.04	15.15	14.60	14.76	14.22	15.07	4.98	4.86	4.85	5.05
K	0.91	1.37	0.92	0.00	0.00	0.00	0.00	0.00	0.00	0.01	0.01	0.01	0.01	0.01	0.02	0.01	0.00	0.00	0.00
Ba	0.00	0.00	0.00	0.00	0.00	0.02	0.02	0.00	0.01	0.01	0.00	0.00	0.00	0.00	0.00	0.00	0.00	0.01	0.00
Sr	0.01	0.00	0.01	0.00	0.00	0.05	0.01	0.00	0.01	0.00	0.02	0.03	0.00	0.00	0.00	0.00	0.00	0.00	0.00
H_2O	22.11	21.45	22.77	24.27	24.02	24.31	24.05	23.56	22.81	22.59	18.15	18.80	17.91	18.38	18.28	23.76	24.29	23.39	23.65
E %*	2.90	2.44	2.63	3.09	3.72	2.83	1.79	2.16	3.59	2.97	4.59	7.16	5.95	7.03	5.97	3.08	5.15	4.10	3.57
Si/Al	2.11	2.11	2.1	1.51	1.49	1.52	1.52	1.49	1.51	1.51	1.48	1.5	1.5	1.49	1.48	1.51	1.51	1.51	1.5

*E%= 100X[Al–(Na + K)–2(Mg + Ca + Sr + Ba)]/[(Na + K) + 2(Mg + Ca + Sr + Ba)]

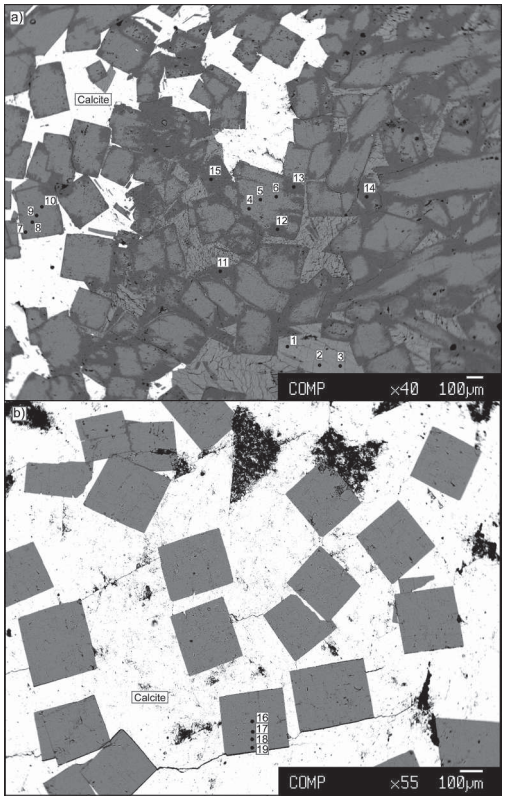

FIG. 5. Back-scattered electron (BSE) images of (a) mesolite crystals replaced by natrolite surrounded by scolecite and calcite (Zone II) and (b) mesolite crystals surrounded by calcite (Zone III).

presence of Ca^{2+} ions during the later stages and the order of crystallization suggests that Ca^{+} ions were being continuously provided to the solution.

ACKNOWLEDGMENTS

The authors thank Dr. G.D. Gatta (Milano) for his valuable criticism of the first version of the manuscript. Dr. D. Ohnenstetter (Nancy) and the anonymous referee are gratefully acknowledged for their comments.

REFERENCES

AKIZUKI, M. & HARADA, K. (1988) Symmetry, twinning, and parallel growth of scolecite, mesolite, and natrolite. *American Mineralogist* **73**, 613–618.

ALBERTI, A., PONGILUPPI, D., & VEZZALINI, G. (1982) The crystal chemistry of natrolite, mesolite and scolecite. *Neues Jahrbuch für Mineralogie - Monatshefte,* 231–248.

ALPASLAN, M. & TEMEL, A. (2000) Petrographic and Geochemical Evidence for Magma Mixing and Crustal Contamination in the Post Collisional Calc-Alkaline Yozgat Volcanics, Central Anatolia, Turkey. *International Geology Review* **42**, 850–863.

ARMBRUSTER, T. & GUNTER, M.E. (2001) Crystal structures of natural zeolites. *In* Natural Zeolites: Occurrence, Properties, Applications (D.L. Bish & D.W. Ming, eds.). *Reviews in Mineralogy and Geochemistry* **45**, Washington, D.C., United States (1–67).

BIRCH, W.D. (1989) Chemistry of Victorian zeolites. *In* Zeolites of Victoria, Special Publication **2** (W.D. Birch, ed.). Mineralogical Society of Victoria, Victoria, Australia (91–102).

BOLES, J.R. & COOMBS, D.S. (1977) Zeolite facies alteration of sandstones in the southland syncline, New Zealand. *American Journal of Science* **277**, 982–1012.

BRECK, D.W. (1974) *Zeolite Molecular Sieves: Structure, Chemistry and Uses*. John Wiley & Sons, New York, United States, 771 pp.

BÜYÜKÖNAL, G. (1986) Major and trace element distribution of the volcanic rocks around Yozgat. *MTA (Maden Tetik ve Arama) Bulletin* **105/106**, 97–111 (in Turkish).

ERDOĞAN, B., AKAY, E., & UĞUR, M.S. (1996) Geology of the Yozgat Region and Evolution of the Collisional Çankiri Basin. *International Geology Review* **38**, 788–806.

GENELI, F. (2011) *Petrology of Eocene volcanism in Central Anatolia: Implications for the early Tertiary evolution of the Central Anatolian Crystalline Complex*. Ph.D. Thesis, Middle East Technical University, 252 pp.

GENELI, F., GÖNCÜOĞLU, M.C., LASSITER, J., & TOKSOY-KÖKSAL, F. (2010) Eocene post-collisional volcanism in the Central Anatolian Crystalline Complex, Turkey: Petrology and Geodynamic significance. 19. Carpathian-Balkan Geological Association. *Proceedings of Geology Balkan* **39(1–2)**, 127–128.

GÖNCÜOĞLU, M.C. (2010) Introduction to the Geology of Turkey: Geodynamic evolution of the pre-Alpine and Alpine terranes. *General Directorate of Mineral Research and Exploration* Monography Series **5**, 66 pp.

GÖNCÜOĞLU, M.C. & GENELI, F. (2008) Eocene volcanism in the Central Anatolian Crystalline Complex: Geochemical indications for a change from post-collision to extension. *Geochimica Cosmochimica Acta* **72**, A318.

GOTTARDI, G. (1989) The genesis of zeolites. *European Journal of Mineralogy* **1**, 479–487.

GOTTARDI, G. & GALLI, E. (1985) Natural zeolites. *Minerals and Rocks* **18**, Springer-Verlag, Berlin, Germany, 409 pp.

GUNTER, M.E. & RIBBE, P.H. (1993) Natrolite group zeolites: Correlations of optical properties and crystal chemistry. *Zeolites* **13**, 435–440.

GUNTER, M.E., KNOWLES, C.R., & SCHALCK, D.K. (1993) Composite natrolite-mesolite crystals from the Columbia River Basalt Group, Clarkston, Washington. *Canadian Mineralogist* **31**, 467–470.

HAY, R.L. (1978) Geologic occurrence of zeolites. *In* Natural zeolites: Occurrence, Properties, Use (L.B. Sand & F.A. Mumpton, eds.). Pergamon Press, Elmsford, New York, United States (135–143).

HAY, R. & SHEPPARD, R. (2001) Occurrence of zeolites in sedimentary rocks: An overview. *In* Natural Zeolites: Occurrence, Properties, Applications (D.L. Bish & D.W. Ming, eds.). *Reviews in Mineralogy and Geochemistry* **45**, Washington, D.C., United States (217–234).

KARAYIĞIT, A.I., ERIS, E., & CICIOĞLU, E. (1996) Coal geology, chemical and petrographical characteristics, and implications for coalbed methane development of subbituminous coals from the Sorgun and Suluova Eocene basins, Turkey. *In* Coalbed Methane and Coal Geology (R. Gayer & I. Harris, eds.). *Geological Society London, Special Publication* **109**, 325–338.

KLAPROTH, M.H. (1803) XV. Chemische Untersuchung des Natroliths. *Ges Naturforsch Freunde Berlin Neue Schriften* **4**, 243–248.

KRISTMANNSDOTTIR, H. & TOMASSON, J. (1978) Zeolites zones in geothermal areas in Iceland. *In* Natural Zeolites: Occurrence, Properties, Use (L.B. Sand & F.A. Mumpton, eds.). Pergamon Press, New York, United States (277–284).

MING, D.W. & MUMPTON, F.A. (1989) Zeolites in soils. *In* Minerals in Soil Environments (J.B. Dixon & S.B. Weed, eds.). Soil Science Society of America, Wisconsin, United States (873–911).

MUMPTON, F.A. (1978) Natural zeolites: a new industrial mineral commodity. *In* Natural Zeolites: Occurrence, Properties, Use (L.B. Sand & F.A. Mumpton, eds.). Pergamon Press, Elmsford, New York, United States (3–27).

NAWAZ, R., MALONE, J.F., & DIN, V.K. (1985) Pseudomesolite is mesolite. *Mineralogical Magazine* **49**, 103–105.

PASSAGLIA, E. (1970) The crystal chemistry of chabazites. *American Mineralogist* **55**, 1278–1301.

PASSAGLIA, E. & SHEPPARD, R.A. (2001) The crystal chemistry of zeolites. *Reviews in Mineralogy and Geochemistry* **45**, 69–116.

TINGLE, T.N., NEUHOFF, P.S., OSTERGREEN, J.D., JONES, R.E., & DONOVAN, J.J. (1996) The effect of 'missing' (unanalyzed) oxygen on quantitative electron microprobe microanalysis of hydrous silicate and oxide minerals. *Geological Society of America, Abstract with Programs* **28**, A–212 pp.

TSCHERNICH, R.W. (1992) *Zeolites of the world*. Geoscience Press, Tucson, Arizona, United States, 563 pp.

TSITSISHVILI, G.V., ANDRONIKASHVILI, T.G., KIROV, G.N., & FILIZOVA, L.D. (1992) *Natural Zeolites*. Ellis Horwood, New York, United States, 295 pp.

Received March 9, 2015. Revised manuscript accepted September 17, 2015.